

NONLINEAR INTERACTION MODELING IN PHOTONIC CRYSTALS

Dana Georgeta POPESCU,¹ Paul STERIAN²

Abstract. *This paper presents several methods for photonic crystals (PCs) characterization which are subsequently applied to realistic systems using specialized software. These methods are Finite Element Method, Plane Wave Method, Finite Difference Time Domain Method, Multipole and Bloch Wave Methods. Based on a full nonlinear system of equations, a nonlinear SHG (Second Harmonic Generation) problem in one-dimensional photonic crystals will be analyzed using Finite Element Method coupled with Fixed Point Iterations. The diagrams resulted after parameter variations are plotted using FlexPDE Professional software. As a result we obtained two maximum intensities of the second harmonic wave within each high index layer, contrasting to the fundamental wave peak. Also a representative band structure using the Plane Wave Method is given.*

Keywords: photonic crystal, finite element method, plane wave method, second harmonic, band structure

1. Introduction

Photonic crystals are periodic dielectric structures which have a band gap that forbids the propagation of radiation within a certain frequency range. This property allows an enhanced control of light effects, otherwise difficult to control with conventional optics.

Photonic crystals are described by Maxwell's equations:

$$\nabla \cdot \vec{E} = \frac{\rho}{\epsilon_0} \quad (1.1)$$

$$\nabla \cdot \vec{B} = 0 \quad (1.2)$$

$$\nabla \times \vec{E} = -\frac{\partial \vec{B}}{\partial t} \quad (1.3)$$

$$\nabla \times \vec{B} = \mu_0 \vec{J} + \mu_0 \epsilon_0 \frac{\partial \vec{E}}{\partial t} \quad (1.4)$$

¹Eng., The Faculty of Electronics, Telecommunication and Information Technology, National Institute of Materials Physics, University "Politehnica" of Bucharest, Romania (dana.popescu@infim.ro).

²Prof., Ph.D., eng. University "Politehnica" of Bucharest, Romania; full member of the Academy of Romanian Scientists (sterian@physics.pub.ro).

where \vec{E} is the electric field strength, \vec{B} is the magnetic flux density, ρ is the charge density, ε_0 and μ_0 are respectively the vacuum dielectric constant and permeability and \vec{J} is the current density.

We can classify these materials with "photonic band gaps" (PBGs) in one-, two- and three dimensional [1], as illustrated in Figure 1.1.

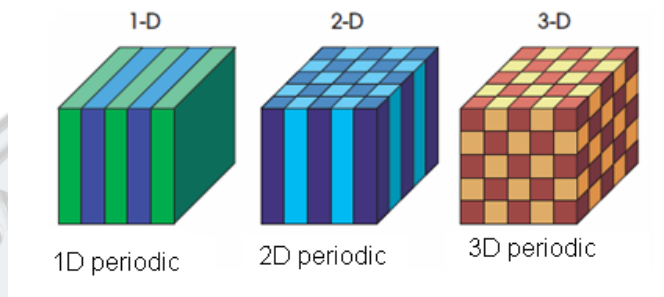


Fig. 1.1. Examples of one-, two-, three-dimensional PCs.
Different colors represent materials with different dielectric constant.

The main goal of this paper is to present some theoretical models: Finite Element Method, Finite Difference Time Domain Method, Plane Wave Method, Multipole Method and Bloch Wave Method and then verify some of them for realistic cases. These techniques are very useful in understanding the special properties of the photonic crystals. In this manner we can predict and explain their behavior without resorting to brute force calculation. At the end, we highlight the utility of FlexPDE Professional and Matlab software in 1D and 2D photonic crystal computer simulations.

2. Methods

2.1. Finite element method in photonic crystals study (FEM)

Using finite element method we can effectively investigate the modes allowed by photonic crystals when imposing periodic boundary conditions to a unit cell of a given material. Such PBG (photonic band gap) materials, restricted at the two-dimensional periodicity, have been successfully fabricated. We can obtain a reduction in complexity (a reduction in processor and memory requirement) for the in-plane propagation modes of photonic crystals using 2D Lagrangian finite elements. The FEM is efficient due to scattered eigensystem matrices and to the discontinuous dielectric constant which is handled in the real space. As an important application of the FEM we can consider the computation of the band structure for many common PC structures. With this numerical FEM technique we can easily and exactly represent the sharp discontinuities in dielectric constant and

solve boundary value problems for many PBG materials. The FEM is also used in meshing the dielectric function profile of the photonic crystals and by solving eigenvalue equation with proper periodic boundary conditions following the Bloch theorem we can calculate the in-plane band structures and in-plane photon density of states (PDOS) of the two-dimensional photonic crystals for the TE and TM modes.

Referring to PC structure the FEM involves breaking down the problem domain into many small elements of simple shape. The equations used are derived from Maxwell's equations that approximate the electromagnetic field over an element. An interpolation function coupled with its coefficients express this approximation of the field. Making a compromise between the quality of approximation and the number of degrees of freedom (the number of function coefficients) we can choose an interpolation function. A good approximation of the true solution might be given by a higher order interpolation function, but this will require a large number of function coefficients thus increasing the computational and storage costs. The function coefficients must be computed for every element after choosing the interpolation function. These coefficients are then stored as elemental matrices, which may be subsequently assembled into global matrices by mapping local to global interpolatory node numbers. So an eigensystem of scattered matrices is formed by these global matrices. Using a subspace iterative technique we can solve this system of equations.

The resulting eigenvalues are the frequencies of the allowed modes with their corresponding eigenvectors representing the field strength at the nodes [2-3].

A highly interesting case is prompted by introducing a defect into an otherwise highly ordered PC structure. The defect could be an alteration of a rods diameter, a variation in the dielectric constant of a rod or complete removal of a rod or rods [4]. The FEM output can certify the effect of these defects, used in controlling the frequency and range of photonic band-gaps.

The modes having a frequency within the range of the band gap can propagate when we introduce a defect into the crystal structure. The defect induced mode is effectively "pinned" by the defect [1] and it cannot propagate through the crystal as it has a frequency within the forbidden range (the light is localized and cannot „escape”).

Generally speaking, the finite element method is a numerical technique used in finding approximate solutions of integral equations, or of partial differential equations (PDE). The solution approached is based on transforming the PDE into an approximate system of ordinary differential equations, or on completely eliminating the differential equation. This system is then integrated numerically using standard techniques such as Euler's method.

In solving PDE, the main challenge consist is finding an equation that approximates the original one. Great care should be paid in order to avoid the accumulation of errors from intermediate calculations and from the input which could make the resulting output meaningless.

We can use FEM for solving PDE over complicated domains, when the desired precision varies over the entire domain, or when the domain changes.

FEM is used in aeronautical, automotive industries, biomechanical, in design and development of some products, in minimizing materials, weight and costs. It allows the detailed visualization of the regions where structures twist or bend and additionally indicates the distribution of displacements and stresses. Also one can construct an entire, refined and optimized design before it is manufactured. FEM design has improved the methodology of the design process and the standard of engineering in many industrial applications [5-9].

FEM benefits include enhanced design, increased accuracy and better understanding of design parameters and other cycles in production.

To illustrate the FEM we considered a nonlinear photonic crystal which offers unique and fundamental methods of enhancing various nonlinear optical processes. In the third part of this paper we used nonlinear Helmholtz equations, which are based on Maxwell's equations, and the corresponding equations of boundary conditions to emphasize the second harmonic effect. The nonlinear problem revealed has a unique solution only if the contribution of the nonlinear susceptibility tensor is not too large. We show that second harmonic generation efficiency can be improved by creating defects in the periodic structure.

2.2. Plane wave method in photonic crystals study (PWM)

Computational modeling of PBG devices has traditionally been approached using plane wave expansion techniques. We can take advantage of the unique properties of PCs with a calculation method necessary to determine how light will propagate through a particular periodic structure. For a periodic dielectric structure we can find eigenfrequencies (the allowed frequencies) for light propagation in all crystal directions being also able to calculate the field distributions in the crystal for any frequency of light. One of the most studied and reliable method is the PWM. It is simple enough to be easily implemented and it was used in some of the earliest studies of photonic crystals [10-12].

Modifying the conventional plane wave expansion method we can enlarge its application region making it suitable for solving the interface problem between vacuum and a semi-infinite PC system. This method has several advantages such as solving the problem of the 'dielectric rods in air' and 'air rods in dielectric', without any restriction on the shapes of the rods and position of cutting plane that

separating the semi-infinite PC region from the air region and we can use all information getting from the complete set of the eigenfunctions of the translation operator, including both the propagating and evanescent modes. So, we can analyze it easier and discuss the phenomena using the well-established knowledge of solid state physics. Additionally, we can easily isolate the finite size effects such as the resonance behavior of the transmittance curve caused by the finite thickness of the PC sample and accurately calculate the transmittance and reflectance for a very thick PC sample.

This numerical method has produced successful results, but has disadvantages such as slow convergence and high demands for computing power and memory.

An example of plane wave method implementation is given in the fourth part of this paper, where we considered two dielectric media with different dielectric constant and we represented the band diagram for a two-dimensional photonic crystal in a triangular lattice. The band structure was computed using PWM consisting in Fourier series expansion of the periodic functions and insertion of these series in the wave equation. By solving the problem we obtain a spectrum of eigenvalues (band diagram) and growth coefficients for Bloch eigenmodes [13].

2.3. Other methods

2.3.1. Finite difference time domain method in photonic crystals study (FDTD)

Another method developed and applied in the analysis and investigation of photonic crystals is the Finite Difference Time Domain method. It is a very general method which does not rely on any assumptions of propagating modes. FDTD method involves a direct discretization of Maxwell's equations, so that the evolution in space and time of a starting field (an incident wave) can be calculated.

In [14] we can find a very helpful overview of the method with rich attention to implementation details and boundary conditions. A drawback of this method is the number of discretization points required for getting stability and accurate results from the algorithm. The time step should be less than the corresponding fraction of the smallest wave period in the problem and the spatial step size should be less than about a tenth of the smallest wavelength.

This limits the size of the problems that can be handled on a given computer, the needed processing time being directly proportional to the number of grid points. We can calculate in this manner a band gap in a PC with an intuitively simple method.

We also can determine the transmission of waves in all directions through the crystal over the range of frequencies of interest. It involves calculations for many angles of incidence and many frequencies over a spatial region.

In many practical application photonic crystals are considered materials with a high refractive index contrast (necessary in order to obtain an appreciable band gap) where waves having frequencies amid the band gap will penetrate for only a few periods, so we can determine its band gap only looking at the transmission through a relatively thin 'block' of PC material.

Also, using a single calculation of FDTD algorithm we can obtain the results for all angles and frequencies.

A drawback is that the method of obtaining frequency spectra by transforming a pulse response from the time domain calculations does not properly accounts for material dispersion which is specified in the frequency domain.

However a method for incorporating material dispersion in FDTD calculations is known [14].

On the other hand, in some cases material dispersion may be neglected with respect to the large 'geometric' dispersion of the periodic PC itself [15].

We can determine the dispersion with FDTD method without performing a formal modal analysis, for a waveguide formed by removing a row of pillars from a photonic crystal consisting of 2D square array of square cross-section high-index pillars in air [4], [10-11], [16].

Also, we can determine the group velocity from the dependence of the frequency.

The exited modes in the waveguide can be separated by spatial Fourier decomposition of the field pattern.

The efficient coupling of waves into a waveguide in a photonic crystal is another practically important issue. Many phenomena can be modeled in PC structures with the FDTD method, some of them being the calculation of a photonic band gaps, resonator-based filters, diffraction effects and waveguide dispersion.

There are limitation of the FDTD such as the difficulty of incorporating material dispersion and the required computer resources.

The illustration of a standard Cartesian Yee cell [17] used for FDTD can be seen in figure 2.1.

We can visualize the electric field strength components (E_x, E_y, E_z) form the edges of the cube and the magnetic field strength components (H_x, H_y, H_z) form the normals to the faces of the cube.

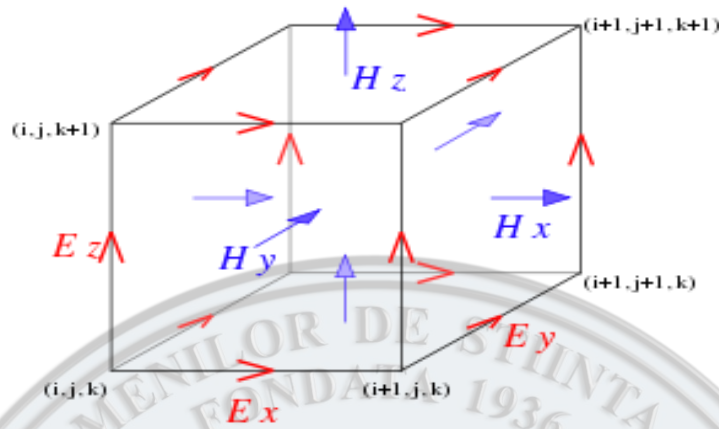


Fig. 2.1. The illustration of a standard Cartesian Yee cell.

Using this model of discretization of Maxwell's equations in time and space one can achieve the analyses over simple optoelectronic devices whose operation are based on the electromagnetic field propagation through periodic media.

FDTD is an intuitive technique based on Maxwell's equations, so one can easily understand how to use it or know what to expect from a fixed model. Being a time domain technique if the source we use is a broadband pulse then one can obtain a response over a wide range of frequencies. This fact can be used in applications when a broadband result is desired or when the resonant frequencies are not known. On the other hand, models with long features are difficult to model in FDTD, because of the large computational domain required.

2.3.2. Multipole method in photonic crystals study (MM)

Multipole methods have evolved as an important class of theoretical and computational techniques in the study of PCs. The MM is a numerical technique used as mode solver, a techniques that is particularly useful in finding modes of microstructured or photonic crystal fibers. It achieves high accuracy and rapid convergence with modest computational resources and it yields both the real and the imaginary parts of the mode propagation constant (provides information about losses), being used for full-vector modal calculations of microstructured fibers and other photonic crystal structures.

The MM is implemented for circular inclusions in freely available software, but it can be extended to noncircular inclusions, too. It can deal with two types of microstructured optical fibers (MOF): air core MOF and a solid core MOF, surrounded by air holes. We can model systems with large numbers of inclusions and the computational overhead is further reduced for structures with discrete rotational symmetries by exploitation of the symmetry properties of the modes. Some convergence problems arise as the spacing between the inclusions decreases

because the method is limited to nonintersecting circular inclusions. Each dielectric boundary in the system is treated as a source of radiating fields in this method. The application of a certain field identity relates the regular field in the vicinity of any scatterer to fields radiated by other scatterers and external sources. The technique has evolved to become an important tool in the solution of dynamic problems involving both finite and periodic systems even if the origins of the method lie in the solution of electrostatic problems for periodic systems.

Additionally, the MM can analytically preserve the symmetry and exploit the natural basis of functions for the scatterers, yielding important physical insight into the scattering processes. The propagation constant in the MM follows from the calculation when the frequency is used as an input parameter. If we are dealing with dispersive media this feature adds a significant advantage because the appropriate refractive indices are known from the outset.

Essential features of MMs for periodic systems are lattice sums, which are sums of terms evaluated at each point of the lattice structure, taking into account its dependence on dimensionality and geometry.

The MM results from considering the balance of incoming and outgoing fields and it allows solving the scattering problem associated with multipole inclusions [18-20]. We consider a single inclusion in the matrix (Fig. 2.1) centered at the origin of the coordinate system O . The field $U(r, \theta + 2\pi) = U(r, \theta)$ is periodic along the angular coordinate. We can expand $U(r, \theta)$ in a Fourier series if we fix r : $U(r, \theta) = \sum_{n \in \mathbb{Z}} f_n(r) e^{in\theta}$, where Fourier coefficients $f_n(r)$ are regular functions of r .

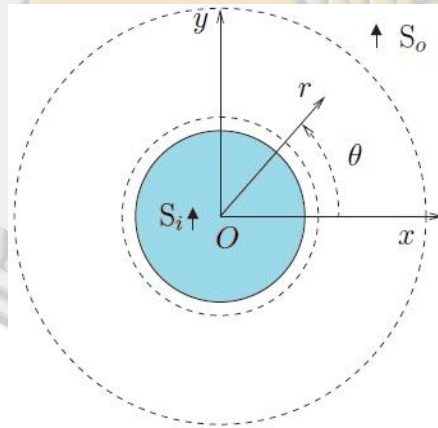


Fig. 2.1. Single inclusion in the matrix where $S_{i,o}$ are sources.

If we consider an inclusion, the field reaching the corresponding region will be scattered. If we consider two inclusions, the incoming field for inclusion 1 results from the superposition of the field radiated from S_o and the scattered field from inclusion 2. The same steps are followed for the incoming field for inclusion 2.

The MM is used in modeling of PCs and MOFs, to design complex/composite devices, such as interferometers, splitters, couplers and to study the radiation properties of sources embedded in such structures. Also, it is useful in studies of finite systems that involve the computation of the local density of states.

2.3.3. Bloch wave method - Method of moments

With MoM (Method of Moments) combined with Bloch wave expansion one can determine the band structure of photonic crystals. This approach is analogous to the spectral domain MoM method and is very efficient in terms of the number of plane wave needed for good convergence, being used for analyzing two-dimensional periodic structures. We can add that the field is expanded in terms of a plane wave spectrum [21] or in a set of eigen function modes (plane wave spectrum in 2D or a Bloch wave in 3D) and an integral equation is enforced on the surface of the scatterers in each unit cell. In the photonic crystal case the unit cell is three-dimensional and in the frequency selective surface case the unit cell is two-dimensional.

The electric field \vec{E} for ideal conducting structures admitting only electric current sources \vec{J} is:

$$\vec{E} = -jk\chi \left[\vec{A} + \frac{1}{k^2} \nabla(\nabla \cdot \vec{A}) \right] \quad (2.3.1)$$

where \vec{A} is the vector potential $\Delta \vec{A} + k^2 \vec{A} = -\vec{J}$ and k is the free space propagation constant and it comes from the derivative in Maxwell's equations.

$$\sum_i I_i \left[\sum_{a,b,c} \frac{\vec{J}_j(-\alpha_a, -\beta_b, -\gamma_c) \vec{G}_{abc} \vec{J}_i(\alpha_a, \beta_b, \gamma_c)}{k^2 - \alpha_a^2 - \beta_b^2 - \gamma_c^2} \right] = 0 \quad (2.3.2)$$

where we consider a cubic lattice in which α only depends on a , β only depends on b , γ only depends on c and:

$$\begin{aligned} \alpha_a &= k_0 \sin \varphi_0 \cos \phi_0 + \frac{2\pi a}{d_x} \\ \beta_b &= k_0 \sin \varphi_0 \sin \phi_0 + \frac{2\pi b}{d_y}, \\ \gamma_c &= k_0 \cos \varphi_0 + \frac{2\pi c}{d_z} \end{aligned}$$

where $k_0 = 2\pi/\lambda$, $d_{x,y,z}$ are the dimensions of the unit cell in the x , y , z directions, λ is the effective wavelength in the crystal, φ_0 and ϕ_0 are the

directions of propagation in spherical coordinates, k_0 represents the propagation constant in the periodic medium, I_i represent unknown weighting coefficients ($\vec{J}(x, y, z) = \sum_i I_i \vec{J}_i(x, y, z)$),

$$\vec{G}_{abc} = \begin{pmatrix} 1 - \frac{\alpha_a^2}{k^2} & -\frac{\alpha_a \beta_b}{k^2} & -\frac{\alpha_a \gamma_c}{k^2} \\ -\frac{\alpha_a \beta_b}{k^2} & 1 - \frac{\beta_b^2}{k^2} & -\frac{\beta_b \gamma_c}{k^2} \\ -\frac{\alpha_a \gamma_c}{k^2} & -\frac{\beta_b \gamma_c}{k^2} & 1 - \frac{\gamma_c^2}{k^2} \end{pmatrix} \text{ is the Green function.}$$

The (2.3.2) equation is very simple to implement and requires only the 3D Fourier Transform of the basis functions to be computed. Computing the band structure of a 3D photonic crystal with this method is as easy as computing transmission and reflection from a 2D periodic surface. Equation (2.3.2) can be used to compute bands in various types of doped and undoped photonic crystals [9-11].

We can assume values for (k_0, φ_0, ϕ_0) and then search for those values of k to compute bands of the crystal, which drive the determinant of the impedance matrix to zero. The (2.3.2) equation can be used to compute bands in various types of doped and undoped PCs [22-24].

3. Second harmonic generation (SHG)

Solving nonlinear Helmholtz equations in combination with finite elements method, presented in section 2, and fixed point iterations reveals a nonlinear optical process called second harmonic generation (SHG).

We can improve the SHG efficiency in nonlinear PCs by adjusting the fundamental wave frequencies and the second harmonic wave to the localized frequencies at the photonic band edge or by creating defects in the nonlinear materials of PCs.

We consider a nonlinear material with periodic structure along the z direction, for $0 \leq z \leq D$ and the nonlinear structure is situated between two linear materials. The nonlinear Helmholtz equations [25-29] are:

$$\frac{d^2 E_1}{dz^2} + (k_0 n_1)^2 E_1 = -k_0^2 \chi_1^{(2)} E_1^* E_2 \quad (3.1)$$

$$\frac{d^2 E_2}{dz^2} + (k_0 n_2)^2 E_2 = -2k_0^2 \chi_2^{(2)} E_1^2 \quad (3.2)$$

where $E_{1,2}$ are the electric fields for the fundamental frequency ω and for the second harmonic frequency 2ω , E_1^* is the complex conjugate, c is the speed of light in vacuum, $k_0 = \omega/c$ is the wave number in vacuum, $n_{1,2}$ are the refractive indices of ω and 2ω , $\chi_{1,2}^{(2)}$ are two second order elements of the nonlinear susceptibility tensors for ω and 2ω .

The coupled nonlinear Helmholtz equation can be solved using the boundary conditions (for $z = 0$ and $z = D$).

The structure we used is formed of 40 dielectric layers and the material is nonlinear. The refractive index alternates between value 1.000 and 1.428 for the fundamental wave and between 1.000 and 1.519 for the second harmonic wave and the layers are $0.25 \mu\text{m}$ and $0.35 \mu\text{m}$ thick. The incident wave is the fundamental mode with $E = 1.0 \text{ MV/m}$ and the nonlinear susceptibility tensor $\chi^{(2),N} = 0.1 \text{ pm/V}$. In figure 3.1a,b we represented the absolute value of the fundamental frequency field and second harmonic field for $\Omega = 0.592$, where a huge amplification of the second harmonic field takes place. The conversion efficiency of the second harmonic should increase considerable because the fundamental frequency is increased with more than one order of magnitude in comparison with the peak value outside the structure. There are two maximum intensities of the SHW within each high index layer in contrast to the fundamental wave peak (the wavelength of the second harmonic signal is half of the pumped wave).

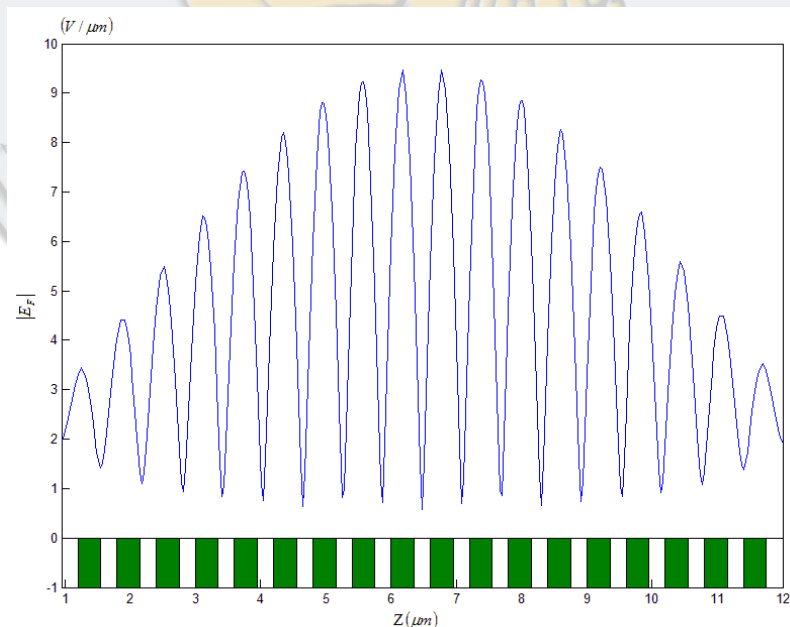


Fig. 3.1a. The absolute value of the fundamental frequency field (fundamental wave).

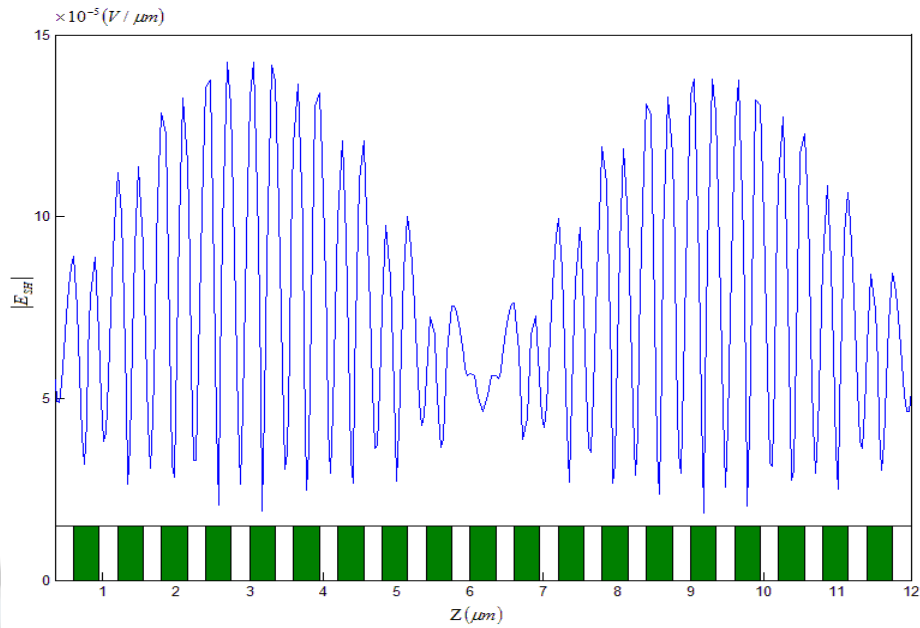


Fig. 3.1b. The absolute value of the second harmonic field (the second harmonic wave).

In figure 3.2a,b are plotted the absolute values of the second harmonic field for a normalized frequency of 0.575 and 0.55, respectively. As we observed in figure 3.1b, in picture plotted below are two maxima intensities of the second harmonic wave in each layer having 1.519 refractive index.

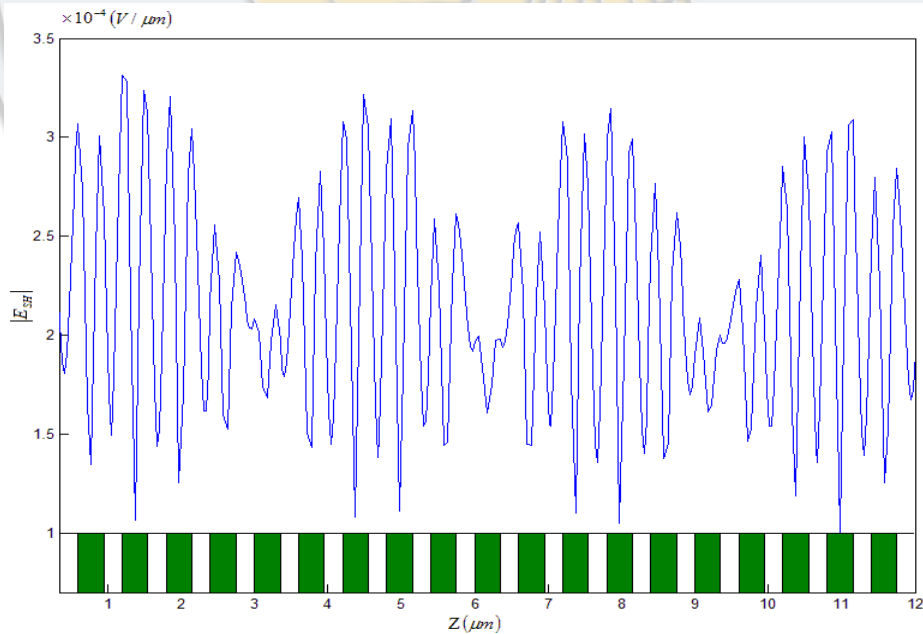


Fig. 3.2a. The absolute value of the second harmonic field (the second harmonic wave for $\Omega=0.575$).

We can see that the frequency decrease of the incident radiation results in significant changes of the shape and intensity of the resulting signal. As expected, for every incoming radiation field having different frequencies, the second harmonic is identified. Their spectral features closely rely on those of the incoming signals, supporting the accuracy of our calculations.

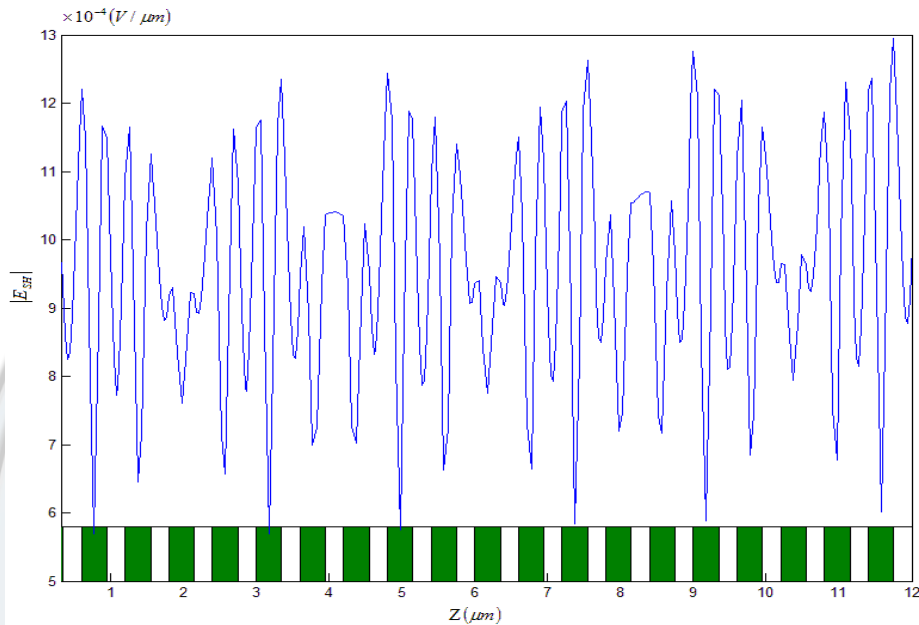


Fig. 3.2b. The absolute value of the second harmonic field (the second harmonic wave for $\Omega=0.55$).

This periodic structure can be studied with FDTD method, too, a method described in the 2.3 section. The structure looks like the one in figure 3.3a.

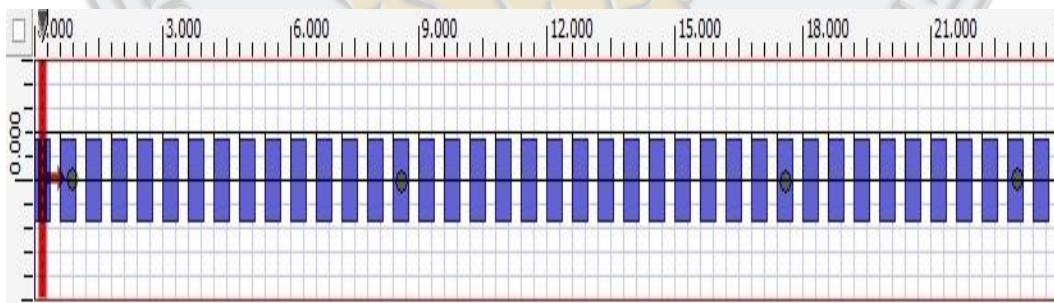


Fig. 3.3a. One-dimensional photonic crystal lattice with 40 dielectric layers and four points of observation along the structure.

Figure 3.3a depicts the periodic structure we used to characterize the SHG in terms described earlier. Figure 3.3b illustrates the way the field propagates along the one-dimensional structure.

We can observe that the field is well collimated within y coordinates and it propagates freely.

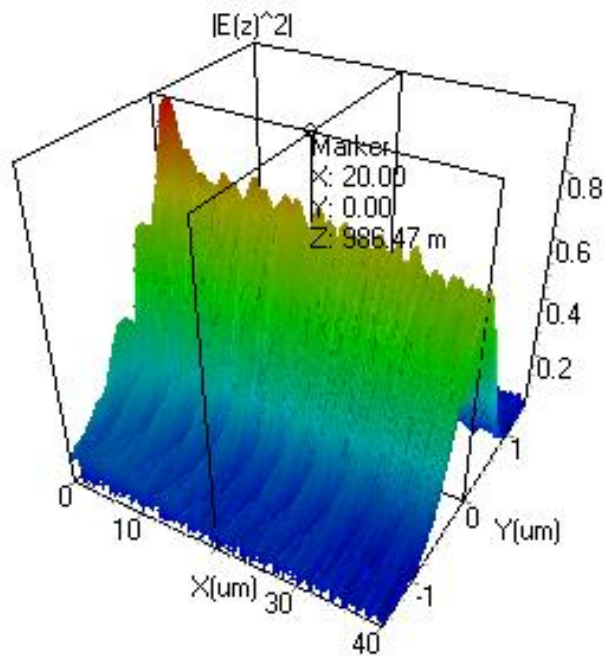
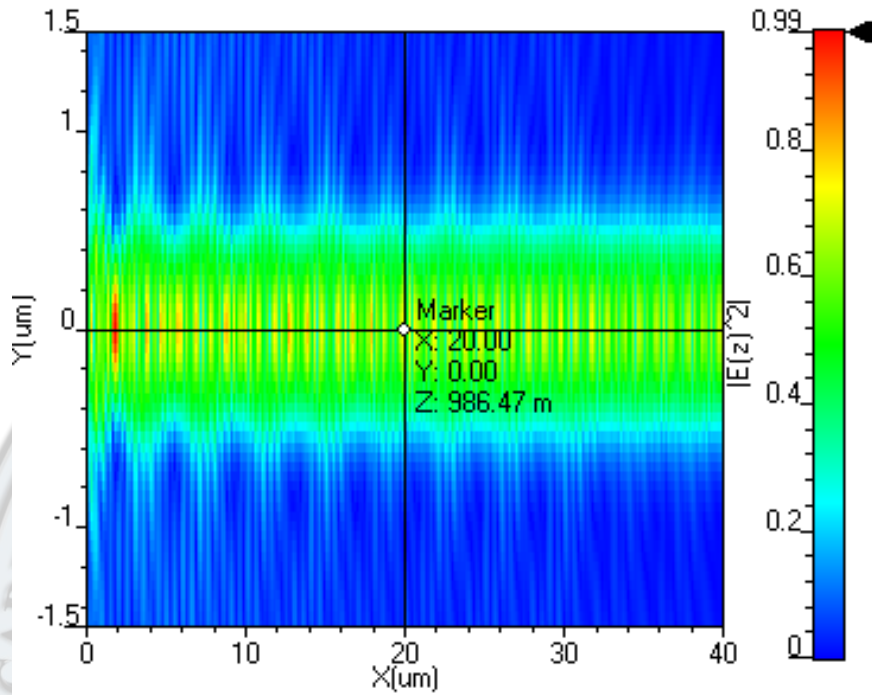


Fig. 3.3b. Field map and other results after simulation.

If we consider a photonic crystal with defect, a structure that we can see in figure 3.4, changing the thickness from 0.304 μm in 0.737 μm of the 15th nonlinear layer (of 29 layers) we obtain a rise of the field in the defect.

The linear layer is considered to be 0.351 μm thick and the refractive index 1.000 and 2.157 for the fundamental wave and 1.000 and 2.237 for the second harmonic wave.

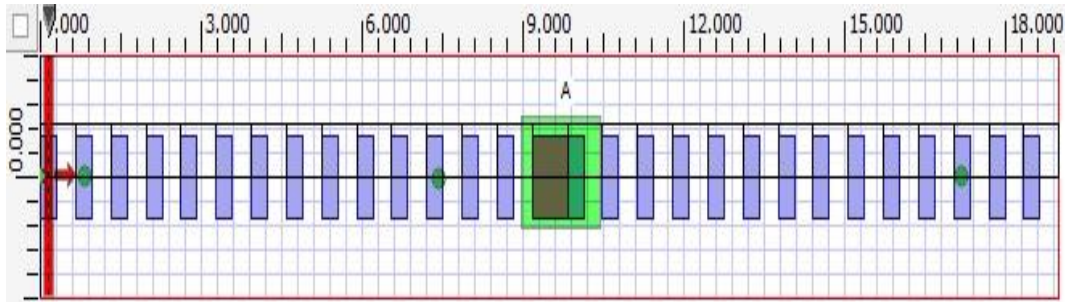


Fig. 3.4. One-dimensional photonic crystal lattice with 29 dielectric layers, three points of observation and one observation area along the structure.

4. The plane wave method implementation in Matlab

We consider two dielectric media with different dielectric constants 1 (air) and 13 (GaAs). The lattice constant is 1.0.

In figure 4.1 are represented calculated photonic band gaps for a two-dimensional photonic crystal consisting of cylinders with circular cross section and infinite length, in a triangular lattice.

We consider plane propagation and two independent polarized states with E and H poles. We can observe a band gap situated between 0.216 μm and 0.325 μm for TE modes (continuous lines) and no band gap for TM modes (dashed lines). In conclusion, this structure has not a total band gap.

To understand the plane wave method presented in section 2 we will expose the convergence problem and the dielectric function representation.

To represent $\varepsilon_r(\vec{r})$ in Fourier space we calculate Fourier coefficients of the inverse dielectric function $1/\varepsilon_r(\vec{r})$:

$$\eta(\vec{G} - \vec{G}') = \frac{1}{\Omega} \int_{\Omega} d^3r \frac{1}{\varepsilon_r(\vec{r})} \exp(-i(\vec{G} - \vec{G}') \cdot \vec{r})$$

where \vec{G} and \vec{G}' are two arbitrary vectors of reciprocal network, Ω is the primitive cell volume.

Considering Maxwell's equations we obtain for the magnetic field:

$$\hat{\Theta}_H \vec{H}(\vec{r}) = \left(\frac{\omega}{c}\right)^2 \vec{H}(\vec{r}), \text{ where } \hat{\Theta}_H = \vec{\nabla} \times \frac{1}{\varepsilon_r(\vec{r})} \vec{\nabla} \times \text{ and } \vec{\nabla} \cdot \vec{H}(\vec{r}) = 0.$$

That is a standard eigenvalues problem, $\Theta \vec{H} = \Lambda \vec{H}$. $\hat{\Theta}_H$ is an hermitic operator and has real eigenvalues.

So, the magnetic field strength \vec{H} becomes:

$$H(\vec{r}) = \exp(i\vec{k} \cdot \vec{r}) h(\vec{r}) \hat{e}_k, \quad h(\vec{r}) = h(\vec{r} + \vec{R}), \quad \vec{h}(\vec{r}) = \sum_{\vec{G}} \vec{h}_{\vec{G}} \exp(i\vec{G} \cdot \vec{r})$$

where \vec{R} is an arbitrary vector of the network, \vec{e}_k is the unit vector which is perpendicular over \vec{k} and parallel with \vec{H} .

So, we obtain:

$$H(\vec{r}) = \hat{e}_k \exp(i\vec{k} \cdot \vec{r}) \sum_{G_i} h(G_i) \exp(i\vec{G}_i \cdot \vec{r}) = \sum_{G_i, \lambda} h(G_i, \lambda) \exp(i(\vec{k} - \vec{G}_i) \cdot \vec{r}) \hat{e}_{\lambda, \vec{k} + \vec{G}_i}$$

where $\hat{e}_{\lambda, \vec{k} + \vec{G}_i}$ is the unit vector perpendicular over $\vec{k} + \vec{G}_i$, $h(\vec{G}_i, \lambda)$ is the amplitude component over the unit vector.

Using Fourier expansion we obtain the matrix form of the PWM equation:

$$\sum_{\vec{G}'} |\vec{k} + \vec{G}'| |\vec{k} + \vec{G}'| \varepsilon^{-1} (\vec{G} - \vec{G}') \begin{bmatrix} \hat{e}_{2\vec{G}} \cdot \hat{e}_{2\vec{G}'} & -\hat{e}_{2\vec{G}} \cdot \hat{e}_{1\vec{G}'} \\ -\hat{e}_{1\vec{G}} \cdot \hat{e}_{2\vec{G}'} & \hat{e}_{1\vec{G}} \cdot \hat{e}_{1\vec{G}'} \end{bmatrix} \begin{bmatrix} h_{1\vec{G}'} \\ h_{2\vec{G}'} \end{bmatrix} = \left(\frac{\omega}{c}\right)^2 \begin{bmatrix} h_{1\vec{G}} \\ h_{2\vec{G}} \end{bmatrix}$$

where $\hat{e}_{1\vec{G}}$ and $\hat{e}_{2\vec{G}}$ are polarization vectors.

And for TM and TE modes the equation are:

$$\sum_{\vec{G}'} |\vec{k} + \vec{G}'| |\vec{k} + \vec{G}'| \varepsilon^{-1} (\vec{G} - \vec{G}') h_{1\vec{G}'} = \left(\frac{\omega}{c}\right)^2 h_{1\vec{G}}$$

$$\sum_{\vec{G}'} (\vec{k} + \vec{G}') (\vec{k} + \vec{G}') \varepsilon^{-1} (\vec{G} - \vec{G}') h_{2\vec{G}'} = \left(\frac{\omega}{c}\right)^2 h_{2\vec{G}}$$

To plot the TE and TM modes in the band diagram we first introduced in the program two dielectric media with different dielectric permittivity 1 and 13.

We considered a two-dimensional periodic network with the network constant $a = 1 \mu\text{m}$. In the elementary cell we have just one "atom" with the radius of $R = 0.48 a$. Knowing the radius and the network constant, we calculated the filling factor.

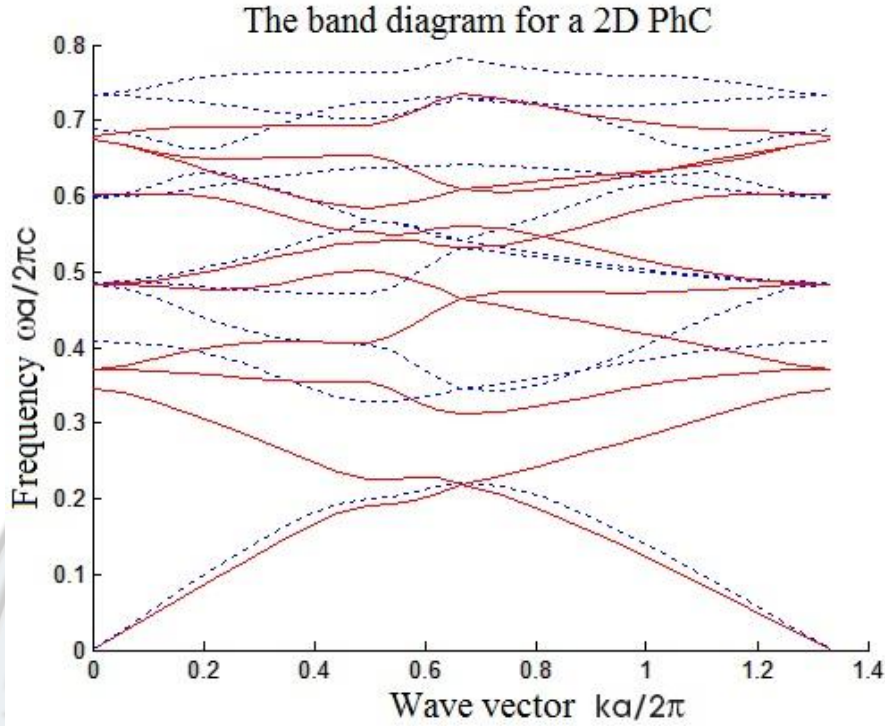


Fig. 4.1. The photonic band gaps for a two-dimensional photonic crystal. The red lines represents TM modes and the dashed ones TE modes. For TE modes we can observe a band gap for 0.216-0.325 frequency interval, and for TM modes we do not have a forbidden band.

Next we introduced the direct lattice vectors \vec{a}_1, \vec{a}_2 : $\vec{a}_1 = a\hat{y}$ and $\vec{a}_2 = a(\sqrt{3}\hat{x} + \hat{y})/2$ and the reciprocal lattice vectors \vec{b}_1, \vec{b}_2 :

$$b_1 = \frac{4\pi}{\sqrt{3}a} \left(-\frac{\sqrt{3}}{2}\hat{x} + \frac{1}{2}\hat{y} \right) \text{ and } b_2 = \frac{4\pi}{\sqrt{3}a}\hat{x}.$$

The direct lattice has a periodicity in the real space. The third part of the code asks us to introduce the n number. We considered a finite lattice with $(2n+1)^2$ elementary cells, even if the two-dimensional network is, theoretically, infinite. The “atoms” positions are given in the direct lattice by the position vectors R and in the reciprocal lattice by G . They are indexed by *count* variable and their number is equal with the number of the plane wave $(2n+1)^2$, meaning that each atom is described by a plane wave.

The bigger the number of the waves, the better the approximation. Knowing the dielectric permittivity lattice which depends of the position vectors of the reciprocal lattice G , we could indicate a k_0 trajectory on the edge of irreducible

Brillouin zone, passing through the high symmetry points Γ, X, M that correspond to k_1, k_2, k_3 vectors. Using the last equations for TE and TM modes we extend them to:

$$TE: \quad M = (\text{real}(k+G) \cdot \text{real}(k+G) + \text{imag}(k+G) \cdot \text{imag}(k+G)) \cdot \text{inv}(\text{eps2})$$

$$TM: \quad M = \text{abs}(k+G) \cdot \text{abs}(k+G) \cdot \text{inv}(\text{eps2})$$

The $\text{eig}(M)$ function calculates eigenvalues of M lattice, which are then sorted with $\text{sort}(\text{abs}(\text{eig}(M)))$ function and at the end we chose only 10 eigenvalues with $\text{sqrt}(\text{abs}(E(1:10)))$. They are saved in variable $\text{freq}(:, \text{counter})$.

We obtained ten energy bands because M lattice depends on the k wave vector. The band structure was finally obtained as depicted in Figure 4.1.

5. Conclusions

We have outlined some methods which may be used for characterizing PC. The techniques considered were Finite Element Method, which is a numerical technique used in finding approximate solutions of integral equations, or of PDE, Plane Wave Method, a method which consist in Fourier series development of the periodic functions and insertion of these series in the wave equation, Finite Difference Time Domain Method, an intuitive technique based on Maxwell's equations which can be used in applications when we desire a broadband result or when we do not know the resonant frequencies, Multipole Method, which results from considering the balance of incoming and outgoing fields and with it one can solve the problem of scattering consisting of multipole inclusions and Bloch Wave Method which helps us determine the band structure of photonic crystals.

Then the second harmonic problem was analyzed using a highly specialized program. We obtained the result that we expected, that meaning two maximum intensities of the second harmonic wave within each high index layer. At the end, we have plotted a band structure of a 2D PC using the Plane Wave Method.

REFERENCES

- [1] J. D. Joannopoulos, R. D. Meade, J.N. Winn, *Photonic Crystals: Molding the Flow of Light*, Princeton, NJ: Princeton University Press, **1995**.
- [2] M. J. Fagan, *Finite element analysis: theory and practice*, Essex, England: Longman Scientific & Technical, NY: Wiley, **1992**.
- [3] Zienkiewicz, R. L. Taylor, *The finite element method*, NY, **1989**.
- [4] D. G. Popescu, P. Sterian, *FDTD analysis of photonic crystals with square and hexagonal symmetry*, submitted to Journal of Advanced Research in Physics, **2011**.
- [5] <http://reference.wolfram.com/applications/structural/FiniteElementMethod.html>.
- [6] http://mms2.ensmp.fr/tribo_paris/lectures/Introduction_FE.pdf.
- [7] E. Bodegom, R. Widenhorn, D. A. Iordache, I. Tunaru, *Study of some additional possibilities and of the evaluation limits of the dark current spectroscopy method*, Annals of the Academy of Romanian Scientists, Series on Science and Technologies of Information, Vol. 4, No. 1, pp. 23-42, **2011**.
- [8] Sterian Andreea Rodica, *Coherent Radiation Generation and Amplification in Erbium Doped Systems*, Adv. in Optical Amplifiers, Paul Urquhart (Ed.), INTECH, Vienna, ISBN: 978-953-307-186-2, **2011**.
- [9] A. D. Petrescu, Andreea Rodica Sterian, P. E. Sterian, *Computer simulations of interaction effects in soliton transmission, for students training*, Annals of the Academy of Romanian Scientists, Series on Science and Technologies of Information, Vol. 1, No. 1, pp. 93-104, **2008**.
- [10] B. Lazar, P. Sterian, *Band gaps in 2D photonic crystals with square symmetry*, Journal of Optoelectronics and Advanced Materials, 12, pp. 810-817, **2010**.
- [11] B. Lazar, P. Sterian, *Band gaps in 2D photonic crystals with hexagonal symmetry*, Journal of Optoelectronics and Advanced Materials, 10, pp. 2882-2889, **2008**.
- [12] B. Lazar, P. Sterian, *The influence of fabrication errors and periodic defects on the width and number of 1D photonic crystals band gaps*, Journal of Optoelectronics and Advanced Materials, 9, pp. 1091-1103, **2007**.
- [13] http://www.phys.ubbcluj.ro/~emil.vinteler/nanofotonica/PWM/Modul2_PWM.pdf.
- [14] A. Taflove, *Computational Electrodynamics: The Finite-Difference Time-Domain Method*, Boston, Artech House Inc., **1995**.
- [15] J. Ctyroky et al., *Bragg waveguide grating as a 1D photonic band gap structure*, Optical and Quantum Electronics, **2001**.
- [16] B. Lazar, P. Sterian, *Photonic crystals resonant cavities. Quality factors*, Journal of Optoelectronics and Advanced Materials, 10, pp. 44-54, **2008**.

- [17] K. Yee, *Numerical solution of initial boundary value problems involving Maxwell's equations in isotropic media*, IEEE Trans. on Antennas and Propagation, 14, pp. 302–307, **1966**.
- [18] K.. Lo, R. McPhedran, I. Bassett, G. Milton, *An electromagnetic theory of dielectric waveguides with multiple embedded cylinder*, J. Lightwave Technol., vol. 12, pp. 396–410, **1994**.
- [19] T. White et al., *Multipole Method for Microstructured Optical Fibers I : Formulation*, J. Opt. Soc. B. vol. 19, pp. 2322-2330, **2002**.
- [20] B. Kuhlmeiy et al., *Multipole Method for Microstructured Optical Fibers II: Implementation and Results* J. Opt. Soc. B., vol. 19, pp. 2331-2340, **2002**.
- [21] Scott, Craig, *The spectral domain method in electromagnetic*, Norwood, MA, Artech House, pp. 149, **1989**.
- [22] Scott, Craig, *Analysis, Design and Testing of Integrated Structural Radomes Built Using Photonic Bandgap Structures*, IEEE Aerospace Conf. Aspen CO, pp. 463 – 479, **1998**.
- [23] Scott, Craig, *Spectral Domain Analysis of Doped Electromagnetic Crystal Radomes Using the Method of Moments*, IEEE Aerospace Conf. Big Sky MT, pp. 2-957 - 2-963, **2002**.
- [24] *Handbook of Mathematical Functions With Formulas, Graphs and Mathematical Tables*, http://apps.nrbook.com/abramowitz_and_stegun/index.html.
- [25] J. Yuan, et al., *Computing for second harmonic generation in one-dimensional nonlinear photonic crystals*, Optics Communications, Vol. 282, Issue 13, pp. 2628-2633, **2009**.
- [26] M. Scalora, M. Bloemer et al., *Pulsed second-harmonic generation in nonlinear, one-dimensional, periodic structures*, Phys. Rev. A, Vol. 56, pp. 3166-3174, **1997**.
- [27] F. Ren, R. Li, et al., *Giant enhancement of second harmonic generation in a finite photonic crystal with a single defect and dual-localized modes*, Phys. Rev. B, vol. 70, Issue 24, pp. 245109-245112, **2004**.
- [28] R. Widenhorn, I. Tunaru, E. Bodegom , D. Iordache, *Study of the numerical modeling of the temperature dependence of the dark current in charge coupled devices*, Annals of the Academy of Romanian Scientists, Series on Science and Technologies of Information, Vol. 3, No. 2, pp. 111-122, **2010**.
- [29] M. C. Piscureanu, *Experimentally proved possibility of generating stable nonlinear directory waves in liquid crystals*, Annals of the Academy of Romanian Scientists, Series on Science and Technologies of Information, Vol. 4, No. 1, pp. 75-78, **2011**.